Available online at www.sciencedirect.com
SCIENCE DIRECT
Nuclear Instruments and Methods in Physics Research A 558 (2006) 106–111
NUCLEAR INSTRUMENTS & METHODS IN PHYSICS RESEARCH Section A
www.elsevier.com/locate/nima

# High-order representation of Poincaré maps

Johannes Grote*, Martin Berz, Kyoko Makino

*Department of Physics and Astronomy, Michigan State University, East Lansing, MI 48824, USA*

Available online 23 January 2006

**Abstract**

A method to obtain DA approximations of Poincaré maps directly from a DA approximation of the flow of the differential equation for certain types of flows and Poincaré sections is presented. Examples of the performance of the method, its computational implementation, and its use for problems in beam physics are given.


*PACS:* 41.85.−p; 05.10.−a; 02.60.Jh; 02.60.Lj

*Keywords:* Poincaré map; Differential algebra

## 1. Introduction

Poincaré maps are a standard tool in general dynamical systems theory for the study of properties of a system under consideration, e.g. the flow generated by an ordinary differential equation. A Poincaré map essentially describes how points on a plane $S_i$ (a Poincaré section) which is transversed by such an orbit $\mathcal{O}$ (the reference orbit) and which are sufficiently close to $\mathcal{O}$ get mapped onto another plane $S_f$ by the flow. A frequent application is the case where $S_i = S_f$, and one of the most prominent applications is the study of asymptotic stability of periodic or almost periodic orbits.

For applications in Accelerator Physics, Poincaré maps are important because the dynamics is usually described in terms of so-called curvilinear coordinates, i.e. an orthogonal coordinate system that is attached to a reference orbit such that one of its axes points in the direction of its velocity, another one in the direction of its acceleration component perpendicular to the velocity, and so on; for details see for example Refs. [1–4]. Instead of solving the ODEs of the original system under consideration with time as the independent variable, the ODEs are transformed such that the new independent variable is the arclength along the reference orbit, and everything is described in terms of the coordinates in the plane perpendicular to the reference orbit.

The benefits of this approach are many: for imaging systems like electron microscopes or other optical systems, the method directly describes how particles originating in the object plane $S_i$ are mapped into the image plane $S_f$, since what matters is the position on this image plane where a detector or, in earlier days, photographic paper or plates are located. Likewise, for dispersive systems, it describes how particles of different energies are mapped into different locations in a detector plane $S_f$. Finally, for large storage rings and circular accelerators, one usually picks one plane $S$ in the ring and assesses long-term stability by studying the Poincaré map for $S = S_i = S_f$.

For many of the conventional particle optical systems, the reference orbit and the dynamics in the corresponding curvilinear coordinates is well-known [1,5]. However, for some of the modern particle optical elements this is not the case, and the mere formulation of the ODEs describing the system under consideration represents a significant problem. Two of the prominent examples of such cases are the dynamics in muon accelerators and storage rings, which are characterized by very large emittances and unusual field arrangements [6–8], and the analysis of modern high-resolution large acceptance particle spectrographs, where the details of the orbits in the fringe field regions of magnets

*Corresponding author.
*E-mail addresses:* grotejoh@msu.edu (J. Grote), berz@msu.edu (M. Berz), makino@msu.edu (K. Makino).
*URL:* http://bt.pa.msu.edu.

0168-9002/$ - see front matter © 2006 Elsevier B.V. All rights reserved.
doi:10.1016/j.nima.2006.01.001

play a prominent role [9–11]. In these cases it is still possible to solve the underlying ODEs in conventional Cartesian coordinates with time as an independent variable; but for the connection with subsequent analysis, it is necessary to transform the results to the form of a Poincaré map.

In the following sections, we will show how this can be obtained using differential algebraic (DA) tools as in Refs. [2,12]. We remark that the proposed algorithm is a part of an extended method which allows the computation of rigorous interval enclosures of the polynomial approximation of the Poincaré map discussed here.

## 2. Review: Essential DA-tools

The DA tools which are necessary to appreciate the method are described in detail in Ref. [2]. However, we wish to review briefly the two most important applications of DA-methods as far as they relate to the problem which is discussed here: the DA-integration method which is employed to obtain high-order polynomial approximations of the flow $\varphi(x_0,t)$ and the functional inversion tools which are necessary in later steps of the algorithm.

### 2.1. DA-integration of ODEs

First, we tackle the problem of obtaining a polynomial approximation of the dependence on initial conditions of the solution of the initial value problem

$$\dot{x}(t)=f(x(t),t),\quad x(0)=X_0+x_0 \tag{2.1}$$

where $f:\mathbb{R}^v\supset U^{\text{open}}\longrightarrow\mathbb{R}^v$ is given as a composition of intrinsic functions which have been defined in DA-arithmetic. As a byproduct this also entails that $f$ exhibits sufficient smoothness to guarantee existence and uniqueness of solutions for all initial conditions. The vector $X_0\in\mathbb{R}^v$ is constant and the midpoint of the domain box $D=[-d_i,d_i]^v$, $i\in\{1,\ldots,v\}$, for the small relative initial conditions $x_0\in D$. Typical box widths $d_i$ are of the order $10^{-2}$–$10^{-8}$. The polynomial approximation $\varphi(x_0,t)$ of the flow of Eq. (2.1) we desire is an expansion in terms of the independent time coordinate $t$ and the relative initial conditions $x_0$, and the representation of this approximation is a so-called DA-vector which stores the expansion coefficients up to a desired order $n$ in a structured fashion.

To achieve the aforementioned goal, we proceed by recalling that the standard procedure of a Picard-iteration yields a polynomial approximation of the solution of (2.1) after repeated application of a Picard-operator on the initial conditions. The iteration in general increases the order of the expansion by one in every step, and since a DA-vector can store coefficients up to a prespecified order $n$, we expect that the iteration converges after finitely many steps in the DA-case.

Accordingly, the Picard-operator in the DA-computation is defined by

$$\mathscr{C}(.):=(X_0+x_0)+\partial_{v+1}^{-1}f(.)$$

where $f$ is computed in DA-arithmetic and $\partial_{v+1}^{-1}$ is the *antiderivation operator*, essentially the integration with respect to the $(v+1)$st variable $t$. It can now be shown that $\mathscr{C}$ is a contracting operator (with a suitable definition of a contraction) and fixed-point theorems exist which guarantee that repeated application of $\mathscr{C}$ on the initial condition $x(0)=X_0+x_0$ will converge to the DA-vector representation of the solution $\varphi(x_0,t)$ of (2.1) in finitely many steps.

### 2.2. Functional inversion using DA-arithmetic

Next we wish to review the actual functional inversion which is employed to obtain the inverse $\mathscr{M}^{-1}$ of a function $\mathscr{M}$, or rather a DA-vector which stores the expansion coefficients of $\mathscr{M}^{-1}$ up to the desired order. Assume we are given a smooth map $\mathscr{M}:\mathbb{R}^v\longrightarrow\mathbb{R}^v$ s.t. $\mathscr{M}(0)=0$ and its linearization $M$ is invertible at the origin. This assures the existence of a smooth inverse $\mathscr{M}^{-1}$ in a neighborhood of the origin. If we write $\mathscr{M}=M+\mathscr{N}$, where $\mathscr{N}$ is the nonlinear part and insert this into the fundamental condition $\mathscr{M}\circ\mathscr{M}^{-1}=\mathscr{I}$, we easily obtain the relation

$$\mathscr{M}^{-1}=M^{-1}\circ(\mathscr{I}-\mathscr{N}\circ\mathscr{M}^{-1})$$

and see that the desired inverse $\mathscr{M}^{-1}$ is a fixed point of the operator $\mathscr{C}(.):=M^{-1}\circ(\mathscr{I}-\mathscr{N}\circ.)$, which proves to be a contraction using a suitable definition of a contracting operator in the DA-picture. Hence the existence of the fixed point $\mathscr{M}^{-1}$ of $\mathscr{C}$ is verified and $\mathscr{M}^{-1}$ can be obtained through repeated iteration of $\mathscr{C}$, beginning with the identity $\mathscr{I}$. Also in this case the iteration converges to $\mathscr{M}^{-1}$ in finitely many steps.

## 3. Description of the method

### 3.1. Preliminary remarks

We begin our discussion by the assumption that the ODE under consideration exhibits a periodic or almost periodic solution $\varphi(X_0,t)$ which starts on a suitable Poincaré section and returns after a period $T$, which has been determined approximately e.g. by a high-order Runge–Kutta-integration. Once such a periodic orbit $\varphi(X_0,t)$ has been identified, we proceed by performing the DA-integration of Eq. (2.1) for one cycle as described in the last section. The goal is to use the new found local dependence on the relative initial conditions $x_0$ to make statements about the qualitative properties of the periodic orbit.

As Poincaré sections, we want to be able to consider as large a class of surfaces as possible. A suitable assumption is that the Poincaré section $S\subset\mathbb{R}^v$ is given in terms of a function $\sigma:\mathbb{R}^v\longrightarrow\mathbb{R}$ as $S:=\{x\in\mathbb{R}^v:\sigma(x)=0\}$. Since the function $\sigma$ also needs to be expressed in terms of elementary functions available in the computer environment for DA arithmetic, it is necessarily smooth, and hence also the surface $S$. This should contain most types of

surfaces which might be of practical interest, in particular, the most common case where $S$ is just an affine plane of the form $S:=\{x \in \mathbb{R}^v : x_1 = c\}$ for some $c \in \mathbb{R}$; here we would have $\sigma(x) = x_1 - c$.

Another condition which needs to be met by $S$ is that the flow is transversal to it for all possible initial conditions $x_0 \in D$. Without this assumption a Poincaré map cannot be defined meaningfully, and we check this condition in the following way: at any point $s \in S$ the gradient $\nabla\sigma(s)$ is perpendicular to $S$, and the direction of the flow is $f(s)$. So we need to ensure that the scalar product $\langle \nabla\sigma(s), f(s)\rangle$ does not change its sign $\forall\, s \in S \cap \varphi(D, T)$. In fact, we will even demand the more stringent condition that $0 \notin [\langle \nabla\sigma(\varphi(x_0, T)), f(\varphi(x_0, T))\rangle]_{x_0 \in D}$, where $[g(x)]_{x \in D}$ denotes a rigorous interval enclosure of a function $g$ over $D$.

### 3.2. Outline of the method

The general goal of the method is to define a Poincaré map which is acting on a suitably chosen section $S$ using only information already available from the DA vector representation of the flow. For every possible initial condition, we wish to derive an expression of the crossing time $t_c(x_0)$ at which the trajectory originating at the said initial value traverses the section $S$, and then reinsert this time $t_c(x_0)$ back into the DA vector $\varphi(x_0, t)$ describing the flow. This yields a polynomial $\varphi(x_0, t_c(x_0))$ only depending on the initial conditions $x_0$ which projects these values almost exactly onto the Poincaré section, up to accuracy restrictions depending on the approximation order. The information about this crossing time is contained in the flow and the geometry of $S$ in an implicit way, hence we need to use suitable tools for functional inversion in the DA context as has been described above. The function $\varphi(x_0, t)$ as such cannot be invertible, since the dimensionality of its domain and range do not even agree. Instead, we will introduce an auxiliary function $\psi(x, t)$ which is substantially easier to handle and yields all relevant results. For $\psi(x, t)$ to be invertible in the first place we need $\psi$ to map into $\mathbb{R}^{v+1}$. This motivates the following:

**Definition 1** (*Auxiliary function for* $\varphi$). Let $\varphi$ be a polynomial representation for the flow under consideration, and let $S$ be a Poincaré section as described above which is traversed by the flow. We then define the *auxiliary function* $\psi : \mathbb{R}^{v+1} \supset D \times I \longrightarrow \mathbb{R}^{v+1}$ by

$$\psi_k(x, t) := x_k \quad \forall k \in \{1, \ldots, v\}$$
$$\psi_{v+1}(x, t) := \sigma(\varphi(x, t))$$

where $I \subset \mathbb{R}$ is open interval s.t. $T \in I$ and $\psi_{v+1}$ is well-defined.

Essentially, $\psi$ contains the crucial part of the flow and is "filled up" with trivial identities in order to achieve invertibility. It can be shown that the map $\psi$ is indeed invertible at the points $\{(x, T) \in \mathbb{R}^{v+1} : x \in D\}$. We can now employ DA inversion tools to manipulate $\psi$ and obtain the inverse $\psi^{-1}(x, t)$. Naturally, because of the identities in $\psi$, also $\psi^{-1}$ will preserve these identities and hence only the component $\psi^{-1}_{v+1}(x, t)$ is nontrivial. Once we have established $\psi^{-1}(x, t)$ we evaluate it at the point $y := (x_0, 0)$ to solve for the crossing time as a function of $x_0$ and set

$$t_c(x_0) := \psi^{-1}_{v+1}(x_0, 0).$$

However, $\varphi(x_0, t_c(x_0))$ still depends on all components of $x_0$, since the crossing time can be specified for the whole domain box $D$. But the Poincaré map $\mathscr{P}$ is supposed to be defined on the surface $S$, a $v-1$-dimensional smooth submanifold of $\mathbb{R}^v$, so one of the coordinates should be redundant. We can perform this restriction of $\mathscr{P}$ to $S$ in the following way:

We assume that $\forall\, x \in \varphi(D, T) \cap S$ the implicit condition $\sigma(x) = 0$ can be stated explicitly as $x_j = \tilde{\sigma}(x_1, \ldots, x_{j-1}, x_{j+1}, x_v)$ for some $j \in \{1, \ldots, v\}$. This can always be done locally, but it is not a very strict requirement that this be true globally in the set $\varphi(D, T) \cap S$. From now on, we will assume wlog that $j = 1$, i.e. $x_1 = \tilde{\sigma}(x_2, \ldots, x_v)$. Then we define the Poincaré map $\mathscr{P}$ by setting $x_{0,1} = \tilde{\sigma}(x_{0,2}, \ldots, x_{0,v})$ and $t = t_c(x_0)$ in $\varphi(x_0, t)$:

$$\mathscr{P}(x_0) := [\varphi(\tilde{\sigma}(.), ., t_c(\tilde{\sigma}(.), .))](x_{0,2}, \ldots, x_{0,v}).$$

As a special case again consider the common instance $S := \{x \in \mathbb{R}^v : x_1 = c\}$ for some $c \in \mathbb{R}$. Then we have $\sigma(x) = x_1 - c$ and thus $\tilde{\sigma}(x_2, \ldots, x_v) = c$ and $\mathscr{P}(x_0) := \varphi(c, x_{0,2}, \ldots, x_{0,v}, t_c(c, x_{0,2}, \ldots, x_{0,v}))$.

### 3.3. Summary of the algorithm

We conclude the presentation of the method by summarizing the algorithmic steps:

(1) Obtain a DA-vector representation of the solution $\varphi(x_0, t)$ for one cycle.
(2) Verify that $0 \notin [\langle \nabla\sigma(\varphi(x_0, T)), f(\varphi(x_0, T))\rangle]_{x_0 \in D}$.
(3) Set up and invert the auxiliary function $\psi$ using DA functional inversion to obtain a DA-vector representation of $\psi^{-1}$.
(4) Evaluate $t_c(x_0) := \psi^{-1}(x_0, 0)$.
(5) Evaluate $\mathscr{P}(x_0) := \varphi(x_0, t_c(x_0))$.
(6) Restrict $\mathscr{P}(x_0)$ to $S$ by replacing $x_{0,1}$ by $\tilde{\sigma}(x_{0,2}, \ldots, x_{0,v})$.

## 4. Example: A muon cooling ring

The method as described above has been implemented in the COSY Infinity environment [13], which offers support for the DA-vector data type and its operations. In fact, COSY even supports the remainder-enhanced DA-vector or Taylor Model data type, which offers rigorous error estimates on the polynomial DA-representation, and we hope to extend the method described above in such a way that also validated error bounds for the Poincaré map can be obtained.

The system we wish to analyze is a problem from accelerator physics, a simple muon cooling ring based on

continuous gas-based cooling and continuous re-acceleration. Focusing is provided by a quadrupole-based FODO system; for details refer to Refs. [7,8,14]. The ODEs governing the motion are described as

$$\dot{x}_1 = x_3$$
$$\dot{x}_2 = x_4$$
$$\dot{x}_3 = x_4 \cdot (1 + k_q r_{xy} + k_h r_{xy}^2) - a \cdot \frac{x_3}{\sqrt{x_3^2 + x_4^2}} + a \cdot \frac{x_2}{\sqrt{x_1^2 + x_2^2}}$$
$$\dot{x}_4 = x_3 \cdot (1 + k_q r_{xy} + k_h r_{xy}^2) - a \cdot \frac{x_4}{\sqrt{x_3^2 + x_4^2}} - a \cdot \frac{x_1}{\sqrt{x_1^2 + x_2^2}}$$

where $a$ describes the cooling and re-acceleration strength, $k_q$ is the quadrupole focusing strength, and $k_h$ is the sextupole strength. In the following simulations, we choose the specific values $a = 0.1$, a focusing scheme based on a 12-fold FODO structure described by $k_q = 10\sin(12t)$, and a sextupole strength of $k_h = 3$.

We consider the initial values $x(0) := X_0 + x_0$ with $X_0 := (0, 1, 1, 0)^T$ and $D := [-10^{-4}, 10^{-4}]^4$. The centerpoint $X_0$ lies on a periodic orbit of the form $\varphi(X_0, t) = (\cos(t), -\sin(t), -\sin(t), -\cos(t))$ and hence has a period of $T = 2\pi$. However, no other orbit originating in the box $X_0 + (D\backslash\{0\})$ is periodic, but instead is slowly pulled towards the invariant solution $\varphi(X_0, t)$ with an asymptotic phase, i.e. $\varphi(X_0 + x_0, t) \to_{t\to\infty} \varphi(X_0, t - \theta(x_0))$ for some phase $\theta(x_0)$.

For this example, we compute the Poincaré map for two planes $S_1$ and $S_2$ before and after one of the 12 FODO cells, so that they form an angle of $2\pi/12$. This map is suitable to be iterated by the COSY beam tracking routines to produce graphics output.

First, we show the results for the crossing time $t_c$ and the components of $\mathscr{P}$ after an 14th order computation with a choice of $a = 0.1$, $k_h = 3$ and $k_q = 10$. The polynomial coefficients are scaled to the phase-space coordinate widths of $10^{-4}$; as a result, each coefficient directly shows the maximum contribution that the corresponding term can make, which helps readability. For the crossing time $t_c$ we obtain

| I | Coefficient | Order | Exponents | | | | |
|---|---|---|---|---|---|---|---|
| 1 | −0.2107121099493938E−01 | 1 | 1 | 0 | 0 | 0 | 0 |
| 2 | 0.9347612653241022E−02 | 1 | 0 | 1 | 0 | 0 | 0 |
| 3 | −0.1201628825073957E−01 | 1 | 0 | 0 | 1 | 0 | 0 |
| 4 | 0.2946295382772426E−02 | 1 | 0 | 0 | 0 | 1 | 0 |
| 5 | −0.1066867771975123E−06 | 2 | 2 | 0 | 0 | 0 | 0 |
| 6 | 0.6346330104788356E−07 | 2 | 1 | 1 | 0 | 0 | 0 |
| 7 | 0.5162610528656688E−06 | 2 | 0 | 2 | 0 | 0 | 0 |
| 8 | 0.2072768191336032E−05 | 2 | 1 | 0 | 1 | 0 | 0 |
| 9 | −0.1221608485172613E−05 | 2 | 0 | 1 | 1 | 0 | 0 |
| 10 | 0.1203023359953680E−05 | 2 | 0 | 0 | 2 | 0 | 0 |
| 11 | 0.9954413063005544E−08 | 2 | 1 | 0 | 0 | 1 | 0 |
| 12 | −0.1069046574180368E−05 | 2 | 0 | 1 | 0 | 1 | 0 |
| 13 | −0.2865490547207094E−06 | 2 | 0 | 0 | 1 | 1 | 0 |
| 14 | −0.1679258946667011E−07 | 2 | 0 | 0 | 0 | 2 | 0 |
| ⋮ | | | | | | | |
| 95 | 0.1412525551591218E−16 | 5 | 1 | 0 | 2 | 2 | 0 |
| 96 | −0.8773781577679656E−17 | 5 | 0 | 1 | 2 | 2 | 0 |
| 97 | −0.8503558663031080E−17 | 5 | 2 | 0 | 0 | 3 | 0 |
| 98 | 0.7544699027997683E−17 | 5 | 1 | 1 | 0 | 3 | 0 |
| 99 | −0.9698655865255742E−17 | 5 | 1 | 0 | 1 | 3 | 0 |

Inserting this into the flow $\varphi(x_0, t)$ and restricting $\varphi(x_0, t)$ to $S$ yields that $\mathscr{P}_1(x_0)$ is given by

| I | Coefficient | Order | Exponents | | | | |
|---|---|---|---|---|---|---|---|
| 1 | 0.5551115123125783E−16 | 0 | 0 | 0 | 0 | 0 | 0 |
| 2 | −0.2475735600348810E−19 | 4 | 0 | 0 | 0 | 4 | 0 |
| 3 | −0.3388692518831476E−19 | 5 | 0 | 3 | 2 | 0 | 0 |
| 4 | 0.3333120608373854E−19 | 5 | 0 | 2 | 3 | 0 | 0 |
| 5 | −0.3552515768008433E−19 | 5 | 0 | 2 | 2 | 1 | 0 |
| 6 | 0.3530916534253391E−19 | 5 | 0 | 1 | 3 | 1 | 0 |

which is indeed zero up to roundoff error, as expected. For the component $\mathscr{P}_2(x_0)$ we get

| I | Coefficient | Order | Exponents | | | | |
|---|---|---|---|---|---|---|---|
| 1 | 1.000000000000000 | 0 | 0 | 0 | 0 | 0 | 0 |
| 2 | 0.4057920121836106E−04 | 1 | 0 | 1 | 0 | 0 | 0 |
| 3 | 0.1403405185907984E−04 | 1 | 0 | 0 | 1 | 0 | 0 |
| 4 | 0.4821854587969232E−04 | 1 | 0 | 0 | 0 | 1 | 0 |
| 5 | −0.6880188908023518E−08 | 2 | 0 | 2 | 0 | 0 | 0 |
| 6 | 0.2218250197573597E−09 | 2 | 0 | 1 | 1 | 0 | 0 |
| 7 | 0.1569399973211117E−08 | 2 | 0 | 0 | 2 | 0 | 0 |
| 8 | 0.3959964998800090E−08 | 2 | 0 | 1 | 0 | 1 | 0 |
| 9 | −0.5900424606672487E−08 | 2 | 0 | 0 | 1 | 1 | 0 |
| 10 | 0.1484090992045488E−08 | 2 | 0 | 0 | 0 | 2 | 0 |
| ⋮ | | | | | | | |
| 36 | 0.2905642684509707E−19 | 5 | 0 | 4 | 1 | 0 | 0 |
| 37 | 0.3555459693963146E−19 | 5 | 0 | 3 | 1 | 1 | 0 |
| 38 | −0.9121533983931736E−19 | 5 | 0 | 2 | 2 | 1 | 0 |
| 39 | 0.8209709912306776E−19 | 5 | 0 | 1 | 3 | 1 | 0 |
| 40 | −0.2773032070261215E−19 | 5 | 0 | 0 | 4 | 1 | 0 |

for $\mathscr{P}_3(x_0)$:

| I | Coefficient | Order | Exponents | | | | |
|---|---|---|---|---|---|---|---|
| 1 | 1.000000000000000 | 0 | 0 | 0 | 0 | 0 | 0 |
| 2 | 0.3916009498009659E−14 | 1 | 0 | 1 | 0 | 0 | 0 |
| 3 | 0.9999999999976929E−04 | 1 | 0 | 0 | 1 | 0 | 0 |
| 4 | −0.6735131658115734E−15 | 1 | 0 | 0 | 0 | 1 | 0 |
| 5 | −0.5073800545630164E−08 | 2 | 0 | 2 | 0 | 0 | 0 |
| 6 | 0.5939776450415390E−08 | 2 | 0 | 1 | 1 | 0 | 0 |
| 7 | −0.1806310552295999E−08 | 2 | 0 | 0 | 2 | 0 | 0 |
| 8 | 0.1202564475352457E−07 | 2 | 0 | 1 | 0 | 1 | 0 |
| 9 | −0.7241099329147064E−08 | 2 | 0 | 0 | 1 | 1 | 0 |

| | | | | | | | |
|---|---|---|---|---|---|---|---|
| 10 | −0.2320522246878191E−08 | 2 | 0 | 0 | 0 | 2 | 0 |
| ⋮ | | | | | | | |
| 47 | 0.4870521605534692E−18 | 5 | 0 | 1 | 2 | 2 | 0 |
| 48 | −0.1330388468272154E−18 | 5 | 0 | 0 | 3 | 2 | 0 |
| 49 | −0.8160539983180998E−19 | 5 | 0 | 2 | 0 | 3 | 0 |
| 50 | 0.9361435018707453E−19 | 5 | 0 | 0 | 2 | 3 | 0 |
| 51 | −0.3132073512809148E−19 | 5 | 0 | 1 | 0 | 4 | 0 |

and for $\mathscr{P}_4(x_0)$:

| I | Coefficient | Order | Exponents | | | | |
|---|---|---|---|---|---|---|---|
| 1 | −0.5551115123125783E−16 | 0 | 0 | 0 | 0 | 0 | 0 |
| 2 | −0.9657136347505140E−04 | 1 | 0 | 1 | 0 | 0 | 0 |
| 3 | 0.5966243086151465E−04 | 1 | 0 | 0 | 1 | 0 | 0 |
| 4 | 0.1191088537008158E−03 | 1 | 0 | 0 | 0 | 1 | 0 |
| 5 | −0.1332746698395360E−07 | 2 | 0 | 2 | 0 | 0 | 0 |
| 6 | −0.1368532466582279E−07 | 2 | 0 | 1 | 1 | 0 | 0 |
| 7 | 0.2399464571937943E−08 | 2 | 0 | 0 | 2 | 0 | 0 |
| 8 | −0.2076327780857213E−09 | 2 | 0 | 1 | 0 | 1 | 0 |
| 9 | 0.3328742850177919E−08 | 2 | 0 | 0 | 1 | 1 | 0 |
| 10 | −0.1163278287959000E−08 | 2 | 0 | 0 | 0 | 2 | 0 |
| ⋮ | | | | | | | |
| 48 | 0.7596735610932742E−18 | 5 | 0 | 1 | 2 | 2 | 0 |
| 49 | −0.7681001402837021E−19 | 5 | 0 | 0 | 3 | 2 | 0 |
| 50 | 0.9040407096077550E−19 | 5 | 0 | 2 | 0 | 3 | 0 |
| 51 | −0.2515146267314533E−18 | 5 | 0 | 1 | 1 | 3 | 0 |
| 52 | 0.5404827028051936E−19 | 5 | 0 | 0 | 2 | 3 | 0 |

In the following we utilize the Poincaré maps just obtained to perform a tracking analysis of the system. Specifically, we use the rescaled maps $\mathscr{P}_2(x_0)$ and $\mathscr{P}_3(x_0)$ and perform beam tracking using the COSY Infinity TR-routine. A total of $n = 6$ particles are launched on the $x$-axis at the positions $n \cdot 4\,\mathrm{cm}$. Figs. (1–3) show the evolution of the motion over 10 turns, 20 turns, and 50 turns, respectively. The cooling action of the system is clearly visible, resulting in the apparent collapse towards the origin. Fig. 4 shows the dynamics displayed in normal form coordinates [2,15], which decouples horizontal and vertical motion and, in the case of the damping, leads to a motion that follows a perfect logarithmic spiral.

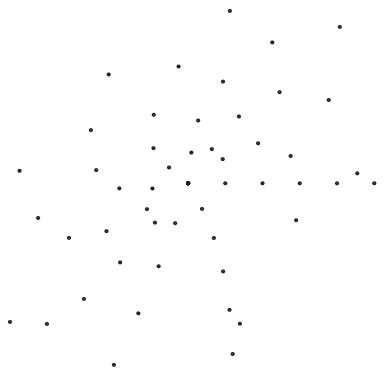

Fig. 1. Tracking of six particles for the first 10 turns in the muon cooling ring.

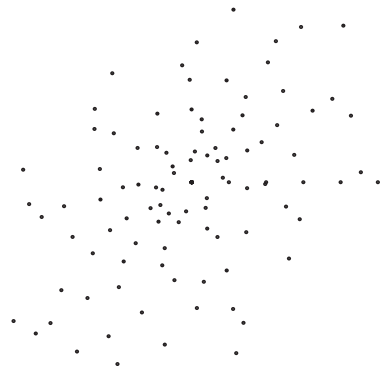

Fig. 2. Tracking of six particles for the first 20 turns in the muon cooling ring.

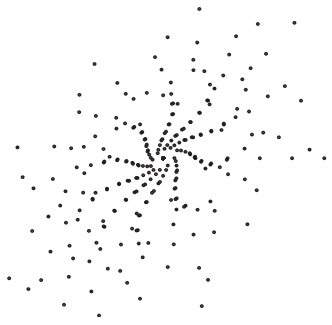

Fig. 3. Tracking of six particles for the first 50 turns in the muon cooling ring.

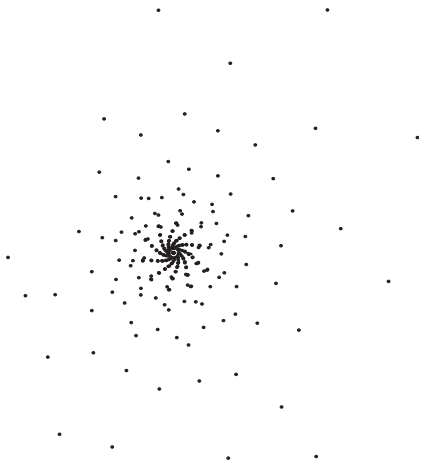

Fig. 4. Tracking of six particles for the first 50 turns in the muon cooling ring, displayed in normal form coordinates.

## References

[1] K.L. Brown, R. Belbeoch, P. Bounin, Rev. Sci. Instr. 35 (1964) 481.
[2] M. Berz, Modern Map Methods in Particle Beam Physics, Academic Press, San Diego, 1999, also available at ⟨ http://bt.pa.msu.edu/pub⟩.
[3] K. Makino, M. Berz, Int. J. Appl. Math. 3 (4) (2000) 421.
[4] M. Berz, K. Makino, Int. J. Appl. Math. 3 (4) (2000) 401.

[5] H. Wollnik, Optics of Charged Particles, Academic Press, Orlando, FL, 1987.
[6] $\mu^+\mu^-$ Collider Collaboration, $\mu^+\mu^-$ collider: a feasibility study, Technical Report BNL-52503, Fermilab-Conf-96/092, LBNL-38946, 1996.
[7] S. Ozaki, et al., for the Muon Collaboration, Feasibility study-II of a muon-based neutrino source, Technical Report 52623, Muon Collider Collaboration, BNL, 2001.
[8] M.M. Alsharo'a, et al., Phys. Rev. ST-AB 6 (2003) 081001.
[9] N. Anantaraman, B. Sherrill (Eds.), Proceedings of the International Conference on Heavy Ion Research with Magnetic Spectrographs, Technical Report MSUCL-685, National Superconducting Cyclotron Laboratory, 1989.
[10] J. Nolen, A.F. Zeller, B. Sherrill, J.C. DeKamp, J. Yurkon, A proposal for construction of the S800 spectrograph, Technical Report MSUCL-694, National Superconducting Cyclotron Laboratory, 1989.
[11] M. Berz, K. Joh, J.A. Nolen, B.M. Sherrill, A.F. Zeller, Phys. Rev. C 47 (2) (1993) 537.
[12] M. Berz, K. Makino, Reliab. Comput. 4 (4) (1998) 361.
[13] M. Berz, J. Hoefkens, K. Makino, COSY INFINITY Version 8.1—programming manual, Technical Report MSUHEP-20703, Department of Physics and Astronomy, Michigan State University, East Lansing, MI 48824, 2001, see also ⟨http://cosy.pa.msu.edu⟩.
[14] K. Makino, M. Berz, C.J. Johnstone, D. Errede, Nucl. Instr. and Meth. A 519 (2004) 162.
[15] M. Berz, Differential algebraic formulation of normal form theory, in: M. Berz, S. Martin, K. Ziegler (Eds.), Proceedings of the Nonlinear Effects in Accelerators, London, 1992, p. 77, IOP Publishing, Bristol.